

5-2015

# Interface Property of Collagen and Hydroxyapatite in Bone

Clint D. Paul

*University of Arkansas, Fayetteville*

Follow this and additional works at: <http://scholarworks.uark.edu/meeguht>

---

## Recommended Citation

Paul, Clint D., "Interface Property of Collagen and Hydroxyapatite in Bone" (2015). *Mechanical Engineering Undergraduate Honors Theses*. 47.

<http://scholarworks.uark.edu/meeguht/47>

This Thesis is brought to you for free and open access by the Mechanical Engineering at ScholarWorks@UARK. It has been accepted for inclusion in Mechanical Engineering Undergraduate Honors Theses by an authorized administrator of ScholarWorks@UARK. For more information, please contact [scholar@uark.edu](mailto:scholar@uark.edu).

Interface Property of Collagen and Hydroxyapatite in Bone

An Undergraduate Honors College Thesis

in the

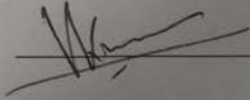
Department of Mechanical Engineering  
College of Engineering  
University of Arkansas  
Fayetteville, AR

by

Clint Daniel Paul

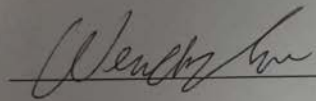
This thesis is approved.

Thesis Advisor:



---

Thesis Committee:



---

---

## Abstract

When looking at bone at the nanoscale, it consists of a matrix of type I collagen and hydroxyapatite (HAP). Type I collagen is the most abundant protein in the body and together with the mineral HAP  $[\text{Ca}_{10}(\text{PO}_4)_6(\text{OH})_2]$  is responsible for most of the structural integrity of bone. Collagen fibrils in bone contain HAP platelets of varying size dispersed between the collagen. The composition of the type I collagen is predicted to play a role in the mechanical properties of the interface.

Our research looks at healthy heterotrimeric collagen and mutated homotrimeric collagen containing three identical chains. Both types of collagen are tested using Steered Molecular Dynamics (SMD) [1] in shearing and peeling directions along the hydroxyl (OH) surface of HAP. The Bell model is also applied to analyze the energy associated with rupturing collagen in shear. The results show that the force required to separate collagen from HAP is not affected by mutation, but the structure of the collagen considerably changes the distribution of hydrogen bonds between collagen-collagen and collagen-HAP interfaces. In shear, homotrimeric collagen forms between 20-40% fewer hydrogen bonds than heterotrimeric collagen. In both shearing and peeling, the number of collagen-water hydrogen bonds increases by roughly 100% before rupture. This research has led to the development of an HAP inspired structure. Currently 3D printed using ABS plastic.

## 1. Introduction

### 1.1. Background:

Genetic mutations during the formation of collagen in the human body cause a number of different types of brittle bone diseases. The most prominent disease of this kind is Osteogenesis Imperfecta (imperfect generation of bone, OI) [2]. People suffering from OI have symptoms varying greatly in severity depending on the type of mutation. The types of OI most closely related to the type of mutation studied here include types II, III, and IV. The most severe being type IV [2]. In this type of OI the collagen formed in the bone experiences residue substitutions in the type I  $\alpha$ -1 or type I  $\alpha$ -2 chains of collagen. Symptoms of type IV OI include extremely fragile bones, stunted bone growth, malformation of teeth, scoliosis, and sclera [2]. At some level, the mutation of collagen plays a crucial role in the structural integrity and growth of bone, but the crucial level and fundamental understanding of the interfaces are yet to be known.

According to the Osteogenesis Imperfecta Foundation, multiple tests are available to help diagnose OI including a Collagen Biochemical Test, Collagen Molecular Test, Recessive OI Test, and multiple prenatal tests. In a Biochemical Test a skin biopsy is taken to look for mutations in collagen proteins formed by skin cells. Molecular Testing requires a blood sample to look for mutations directly at the gene sequencing level. Other tests use skin biopsy samples, blood tests, or ultrasound to detect the presence of OI [3]. From these tests and research into OI, “over 800 different mutations have been identified so far as causes for OI” [3]. When picking exact mutations to simulate, it is important as a first step to pick the most severe mutations as a baseline to map out the differences caused by that mutation. That is why this research focuses on the extreme case of a homotrimeric type I  $\alpha$ -1 collagen molecule. The significance of the homotrimeric mutation is derived from the nature of its composition. The type I  $\alpha$ -2 chain of the collagen is completely replaced by a type I  $\alpha$ -1 chain. Looking at the effects this mutation has on

the collagen-HAP system at the nanoscale provides great insight into understanding OI more fully.

### 1.2. Bone Structure:

Bone consists of a complex hierarchical system that on its own expresses amazing characteristics of strength and flexibility. This biological hierarchy at the highest scale consists of a strong outer compact layer with a spongy interior. At near microscale, the compact bone is made up of osteons and Haversian canals [4]. Inside the osteon system at the microscale there are multiple arrangements of fibers. Below is a figure showing these structures down to the fiber level.

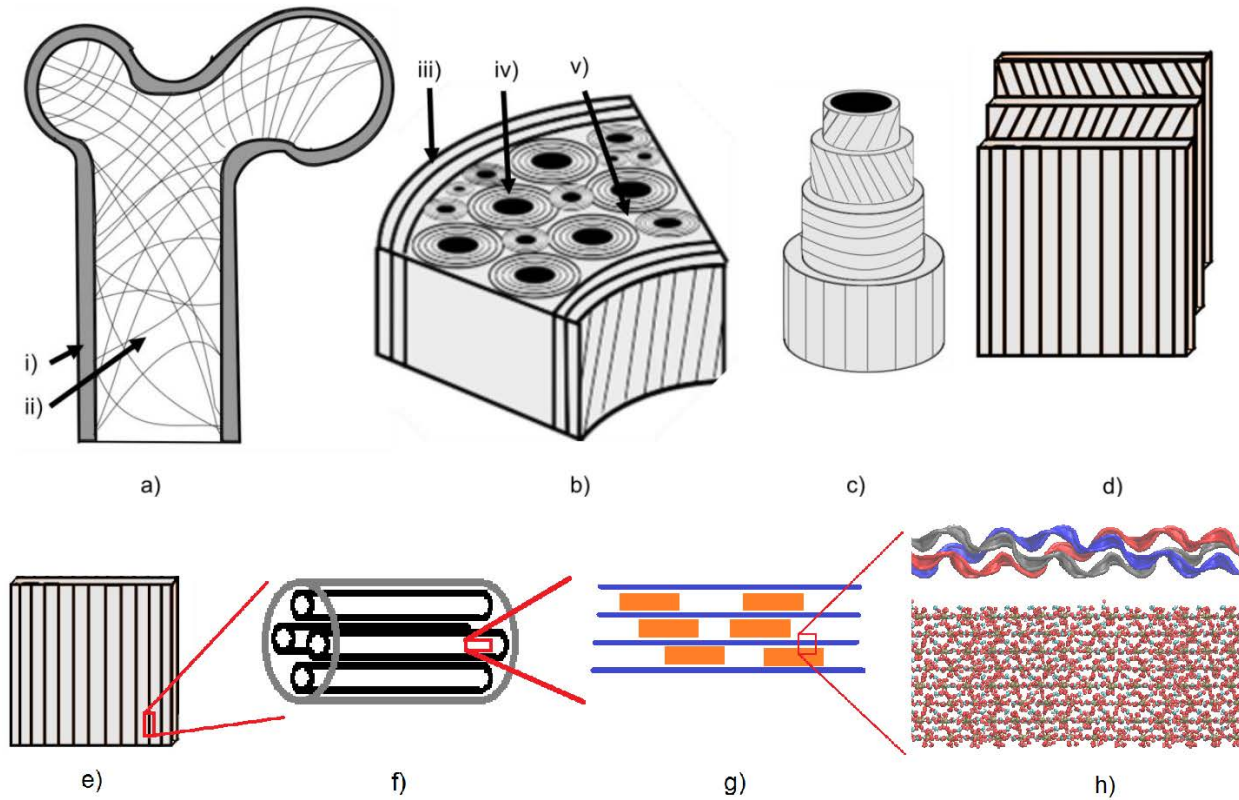


**Figure 1: Bone Structure: a) Basic Structure ~15 cm i) Compact Bone ii) Spongy Bone b) Structure of Compact Bone ~5 cm iii) Circumferential Lamella iv) Osteon System v) Interstitial Lamella c) Osteon System ~ 100  $\mu\text{m}$  d) Structure of Lamellae ~50  $\mu\text{m}$  e) Single Lamellae f) Fibril Arrays ~10  $\mu\text{m}$  g) Mineralized Collagen Fibrils ~1  $\mu\text{m}$  h) Collagen-HAP Interface ~300 nm**

Expanding the scale down further shows the fibers from d) in the figure above, made up of fibril arrays. These fibril arrays consist of a matrix of organic collagen and the mineral apatite [4]. The Lamellae fibers (d) are made of small fibrils (f). These small fibrils are made up of an even smaller complex matrix of collagen and apatite (g). The bottom right panel (h) takes a look at the interface between a segment of one tropocollagen molecule and the surface of HAP. HAP platelets range in size from 1 to 7 nm in thickness, 15 to 200 nm in length, and 10 to 80 nm in width [5, 6, 7, 8]. Collagen forms in lengths of about 300 nm and diameters of 1.5 nm [4].

### 1.3 Objectives:

It is important to understand the mechanical properties of the collagen-HAP interface at the nanoscale, because research shows how a change in mineral density at this level greatly affects the macroscale properties of bone [9]. The goal of this research is to uncover whether or not mutated collagen plays a direct role in the mechanical properties of the interface by itself. The scope of this research does not include the process of forming mutated collagen on the surface. By using SMD, we hope to learn more about the mechanical properties of solvated collagen along the surface of HAP crystals. SMD analysis provides valuable information about the hydrogen bonds associated with the collagen-HAP system. This information can be used by the Bell model to predict the energy barrier for several mechanisms [10, 11, 12]. We hope for the results of this research to inspire the development of 3D printed materials based on the collagen-HAP system.

## **2. Theory**

### 2.1 Tropocollagen Molecules

As stated in section 1.2, collagen forms at lengths of about 300 nm in the collagen-HAP matrix [4]. These long collagen molecules contain thousands of residues, which would be too computationally expensive to atomistically simulate in a full-scale collagen-HAP matrix. The collagen used in these simulations are modeled after real type I  $\alpha$ -1 and type I  $\alpha$ -2 chains of a common house mouse (*mus musculus*) and equilibrated in earlier work using an NPT ensemble [13, 14, 15]. The two chains were then reduced to 57 residues each to reduce computational costs. Ideal collagen consists of a Gly-Pro-Hyp triplet (Glycine-Proline-Hydroxyproline), but in nature the only reoccurring member of this triplet is Gly. The Pro and Hyp positions in the chains are often substituted by other common residues. The truncated chains hold the same composition as the full length chains. Full information about the construction of this molecule can be found in reference [13].

For the simulations considered here, the protein data bank (PDB) files associated with the heterotrimeric and homotrimeric molecules are completed by creating compatible protein structure files (PSF) for each molecule using Visual Molecular Dynamics (VMD) [16]. The N-terminus of each chain is capped with an acetyl group (ACE), while the C-terminus is capped with trimethylamine (CT3) to produce charge neutrality across the entire chain.

### 2.2 Hydroxyapatite Crystal

The hydroxyapatite mineral used in this research is made up of hexagonal unit cells containing 44 atoms with the lattice parameters:  $a=9.4241\text{\AA}$ ,  $b=9.4241\text{\AA}$ ,  $c=6.8814\text{\AA}$ ,  $\alpha=90^\circ$ ,  $\beta=90^\circ$ , and  $\gamma=120^\circ$  [17]. These unit cells are then replicated 24 times along the a-axis, 4 times along the b-axis, and 4 times along the c-axis. The collagen is placed on the OH surface of the HAP because of its negative charge. This allows more hydrogen bonds to form via the increased donors and receptors [18].

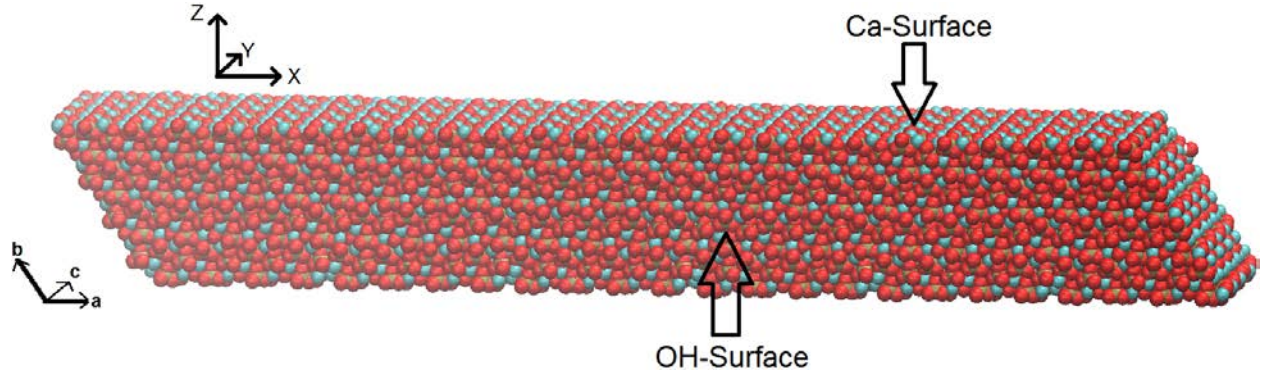


**Figure 2: Diagram of HAP Crystal. Surfaces are labelled accordingly. The a, b, and c axes are based on the HAP lattice parameters while the Cartesian coordinates are associated with the simulated system.**

### 2.3 *Force Fields*

This system is modeled using a modified CHARMM force field originally found in reference [18], because it has been tested to simulate collagen-HAP systems as shown in [18] and [15]. Included in the force field parameters are quantum mechanical calculations derived for hydroxyproline (Hyp), which is found in collagen, but not in other proteins [19]. Nonbonded parameters were originally calculated using a Born-Mayer-Huggins model [20, 21]. This force field has been validated in previous works, [18, 20, 21, 22, 23].

Because this system equilibrates with an unsolvated collagen and later with a solvated collagen, two modified CHARMM force fields are used. The force field for the unsolvated collagen (stated above) has a Coulombic energy that varies with  $\frac{1}{r^2}$  and is thus a dielectric term that varies with distance. When water is added to the system, explicit water molecules must be accounted for in the Coulombic energy by taking away one of the  $\frac{1}{r}$  terms to have the energy drop off linearly with distance [1]. This change is important in simulating solvated biomolecules. Throughout each simulation, Lennard-Jones and Coulombic interactions are calculated by the modified CHARMM fields by ramping energy and force smoothly to zero between the inner and outer cutoff regions of 8Å and 10Å. This has been validated in [1, 15].

### 2.4 *Bell Model*

The Bell model is a theoretical model that combines known parameters of certain bonds and angles with the results of a Molecular Dynamics (MD) simulation to calculate the energy barriers of said bonds [10, 11, 12]. In this study we apply the Bell model to the rupturing of the hydrogen bonds. This allows us to relate a force-displacement to the energy associated with a mechanism. For example, this can be applied during an MD simulation where multiple bonds are broken and new states of equilibrium are reached. The equation for the Bell model used in this study is given [11] as

$$F = \frac{k_B T}{x_b} \ln \left( \frac{V}{\omega_1} \right) + \frac{E_{b1}}{x_b} \quad (1)$$

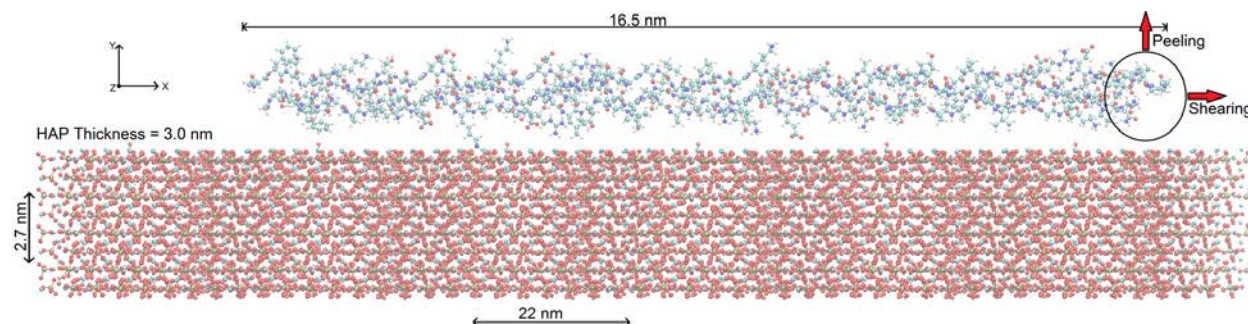
where,  $F$  is the force during rupture,  $k_B$  is the Boltzmann constant,  $T$  is the absolute temperature of the system,  $x_b$  is the slip distance,  $V$  is the loading rate,  $\omega_1$  is the natural frequency of a

hydrogen bond, and  $E_{b1}$  is the energy barrier of the bonds. Without the Bell model, these energy barriers cannot be determined, as the only variable is force, but knowing the temperature, natural frequency of bonds, and pulling velocity allows us to apply the Bell model to estimate the energy barriers associated with each mechanism.

### 3. Methods

#### 3.1 Unsolvated Equilibrium

The coordinates and bond information of each atom/molecule are stored in the PDB and PSF files created earlier (see section 2.1). All simulations are conducted using LAMMPS [1] with a 1.0 fs timestep and all processes are identical for heterotrimeric collagen and homotrimeric collagen. This system is minimized by LAMMPS using two different methods. The first is the conjugate gradient while the second is the steepest descent method. After this minimization process, the system is equilibrated under an NVE ensemble using a Langevin thermostat over 125 ps ramping the temperature from 250 K to 300 K. The bottom single layer of calcium phosphate in HAP is held fixed, while the system is equilibrated again at 300 K for 50 ps. Equilibrium is confirmed by checking the Root Mean Square Distance (RMSD) using VMD [16]. The final frame of the unsolvated system is used as the starting frame for the solvated system.



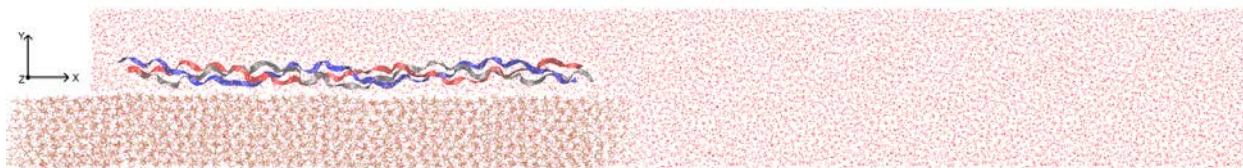
**Figure 3: Diagram of the Collagen-HAP System**

Figure 3 above shows a diagram of the unsolvated system. The HAP is positioned so that the Ca-rich surface is normal to the z-axis, while the OH-rich surface is normal to the y-axis. As shown in the top-right of figure 3, “Peeling” in this report refers to pulling along the y-axis, while “Shearing” refers to pulling along the x-axis.

#### 3.2 Solvated Equilibrium

After the equilibration of the unsolvated system, a box of water molecules using the TIP3 model is added using VMD [16] around the collagen and extended in the predicted trajectory of the collagen during SMD simulations. For the system where shearing is tested, water is added in a  $41 \times 5.5 \times 3.0 \text{ nm}^3$  box extending 23 nm in front of the predicted shearing trajectory. Along with this 23 nm lead, at least 0.8 nm of water is placed around the collagen to ensure consistent solvation.





**Figure 4: Box of water added to system prepared for shearing**

As shown in the figure above, more than the entire length of the collagen was predicted to uncoil and shear off the surface in this test. The system setup for peeling is solvated using the same method as above, except with a box of water extended along the y-axis to ensure full solvation during the simulation. The box of water added for the peeling scenario extends 11 nm above the top of the equilibrated collagen as shown in the figure below.

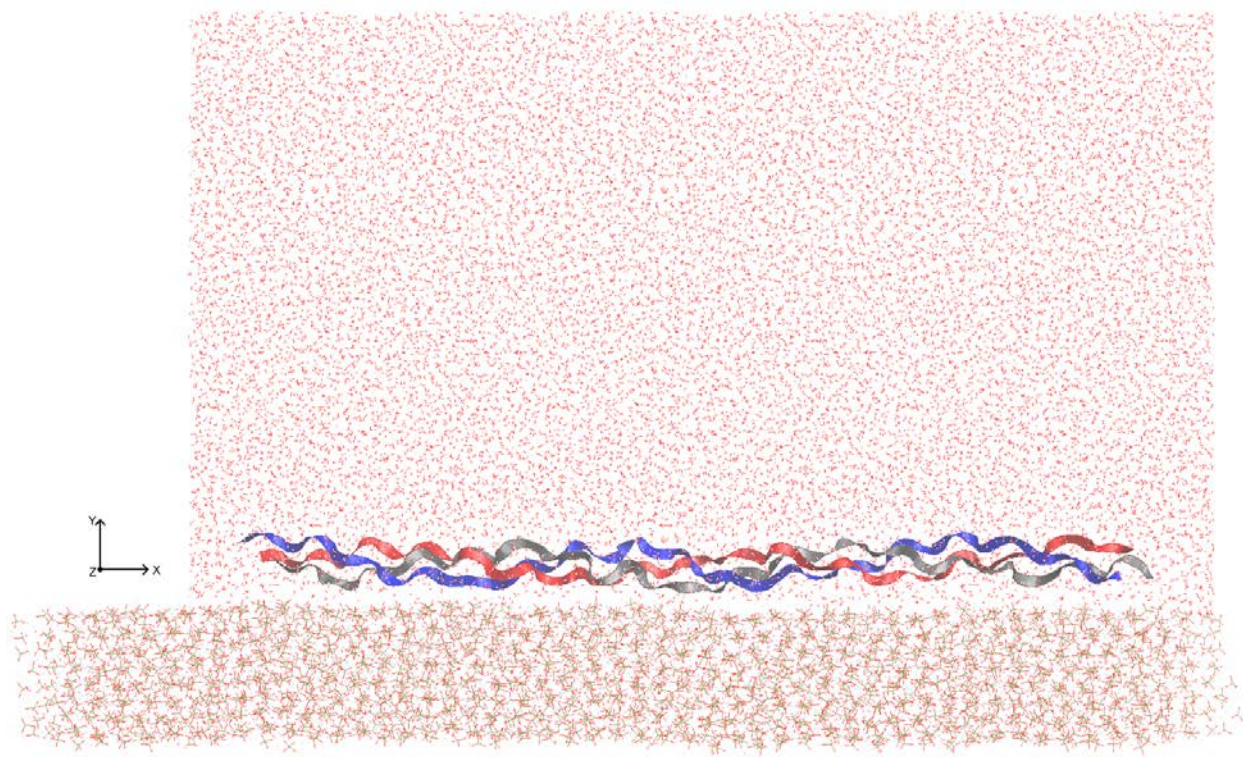


**Figure 5: Box of water added to system prepared for peeling**

As can be seen in the figure above, water is added to give the collagen enough room to separate from the HAP considerably before escaping the water box, but not enough water is added to maintain full solvation for full separation. This decision was made to reduce the computational time required to simulate the system. Both of the systems each contain about 75,000 atoms and require simulation times on the order of weeks using 12 parallel 16-core processors.

As stated above, both systems are minimized and equilibrated using the same parameters as before (see section 3.1) with the only difference being a slight change in the modified Coulombic force field. Once explicit water has been added to the system, the Coulombic energy equation is modified to vary linearly with distance as opposed to an inverse squared relation for

the unsolvated collagen. After the solvated system has been verified at an equilibrium state (once again checked using RMSD) the system is setup to run under SMD [1] calculations.

### 3.3 Steered Molecular Dynamics

Steered Molecular Dynamics (SMD) works by tethering a virtual spring to an atom or group of atoms and pulling the other end of the spring at a constant velocity (or constant force, not used here) [1]. Here, one end of the spring is tethered to the final  $C_\alpha$  atom of each chain. By tethering the spring to three identical atoms, SMD effectively normalizes the masses of the atoms and sets the tethered point to the center of mass of the atoms. The untethered end of the spring is positioned at the same location as the center of mass to ensure zero initial force. Then, depending on whether or not we want to shear or peel the collagen we set the untethered end of the spring to pull at a constant velocity along that axis. The velocity parameter picked here is set to  $0.00001 \frac{\text{\AA}}{\text{fs}}$  or  $(1 \frac{m}{s})$ . This velocity has been tested on collagen-HAP systems and validated in previous works [15, 18, 24]. The spring constant is set to  $10 \frac{\text{kcal}}{\text{mol}-\text{\AA}^2}$  or  $(\sim 6.95 \frac{N}{m})$ , also validated in [15, 18, 24].

### 3.4 Post-Processing

All systems are visualized using VMD [16] along with calculating RMSD, solvating the systems, creating PSF files, and computing hydrogen bonds. Calculating hydrogen bonds using VMD requires a cutoff-distance and cutoff-angle. As previously used successfully in [9, 15, 18], these parameters are set to  $3.5\text{\AA}$  and  $30^\circ$  respectively. MATLAB is used to process results and produce plots for force vs. displacement profiles and hydrogen bond vs. displacement profiles. The displacement distance used in all calculations is the displacement of the untethered end of SMD's virtual spring. The stiffness is calculated at low displacement regions before any bonds have broken (around 10% displacement).

The Bell model is applied using the force vs. displacement plots and known parameters about hydrogen bonds.

$k_B$	$1.380 \times 10^{-23} \frac{J}{K}$
$T$	300K
$V$	$1 \frac{m}{s}$
$\omega_1$	$1 \times 10^{13} Hz$

**Table 1: Constants  $k_B$ ,  $T$ ,  $V$ , and  $\omega_1$  used in the Bell Model**

The table above lists the constants and their units used in the Bell model. Once the energy barrier is calculated, it is transformed into atomistic statistical units of  $\frac{\text{kcal}}{\text{mol}}$ . The force and rupture length are determined from the SMD simulations.

## 4. Results and Discussion

### 4.1.1 Shearing of Heterotrimeric and Homotrimeric Collagen-HAP

We simulate the shearing systems using SMD for approximately 57 ns. During this time the forces reach 300 nN before the homotrimer collagen uncoils. This is shown below in figure 6.

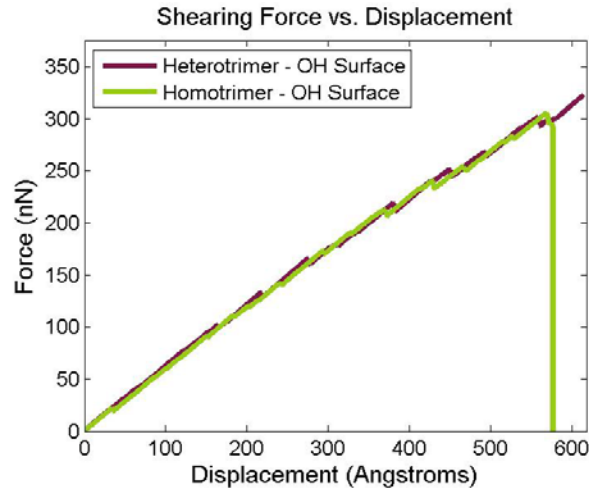


**Figure 6: Force vs. Displacement of Heterotrimeric and Homotrimeric Collagen**

Figure 6 above shows the force vs. displacement for the shearing system. As can immediately be seen in the figure above, the presence of mutated collagen has no effect on the overall trajectory of shearing displacement. This has been predicted in an earlier work [25] where different mutations at higher scales were shown to offer little difference in stress vs. strain. The homotrimeric collagen ruptures from the surface well before heterotrimeric collagen. Looking at low displacements provides us with insight into the stiffness of the interface and information about the first bonds that break.

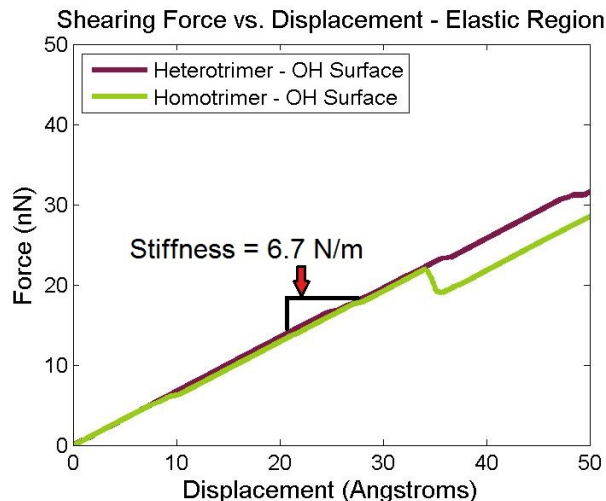
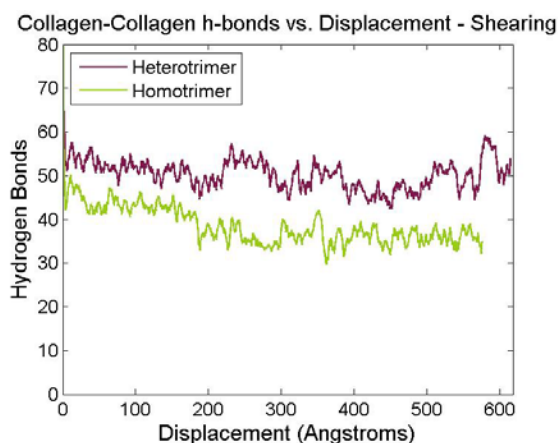


**Figure 7: Force vs. Displacement in Elastic Region of Shearing System**

As shown above in figure 7, both collagen molecules have a nearly identical stiffness of  $6.7 \frac{N}{m}$ . This is important to our initial predictions, because it shows that in the elastic region there

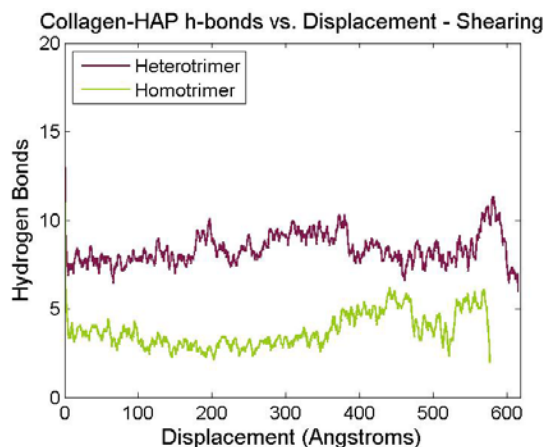
is little to no difference in the way that homotrimeric collagen interacts with HAP. Oddly, when comparing figure 6 with figure 7, even though homotrimeric collagen experiences the first bond break, heterotrimeric collagen experiences more slips that appear to release much more energy.

Force-displacement plots by themselves don't capture the full picture in explaining the similarities and differences between how homotrimeric collagen interacts with itself and the surface of HAP. Below we investigate the role that hydrogen bonds play throughout the SMD simulation.



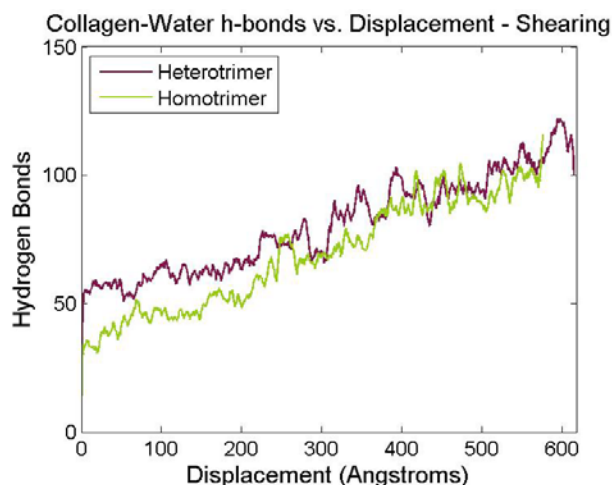
**Figure 8: Collagen-Collagen Hydrogen Bonds vs. Displacement for Shearing**

Figure 8 above shows the plot of collagen-collagen hydrogen bonds formed during the SMD simulation. It is interesting to note that the homotrimeric collagen consistently forms about 20% fewer bonds with itself than heterotrimeric collagen until about 220 Å displacement when the gap grows to a maximum of almost 40%. This shows that the composition of homotrimeric collagen reduces the probability of forming hydrogen bonds within itself, yet it still maintains a nearly identical force vs. displacement profile to that of heterotrimeric collagen. The forces must be coming from somewhere else. Below we look at the hydrogen bonds formed between the collagen and HAP.



**Figure 9: Collagen-HAP Hydrogen Bonds vs. Displacement for Shearing**

Figure 9 above shows the plot of hydrogen bonds formed between the collagen and HAP during the SMD simulation. As interesting as the results from figure 8, the bonds formed between the collagen and HAP for homotrimeric collagen starts out about 50% lower than heterotrimeric collagen with this gap increasing up to nearly 70% after 250 Å displacement. Then the gap closes around 400 Å. The figure below takes a look at the hydrogen bonds formed between the collagen and water.



**Figure 10: Collagen-Water Hydrogen Bonds vs. Displacement for Shearing**

The figure above shows the hydrogen bonds formed between the collagen and water as the collagen is sheared using SMD. As expected, as both collagen molecules start uncoiling they start forming more bonds with the water. This is caused by an effective increase in surface area of the collagen through exposed atoms. Interestingly, homotrimeric collagen forms fewer hydrogen bonds overall, yet has a nearly identical force vs. displacement trajectory. This implies that water indirectly has an effect on the trajectory of collagen through water-water hydrogen bonds. Both molecules are experiencing the same TIP3 water model and homotrimeric collagen forms fewer hydrogen bonds overall, yet they experience the same force vs. displacement.

#### 4.1.2 Applying Bell Model to Shearing System

To apply the Bell model to this system we need to look at locations where the collagen has multiple hydrogen bond ruptures and slips. The most interesting locations for this include the first slip of the simulation and the final large slip. Below we calculate the energy barriers at these locations.



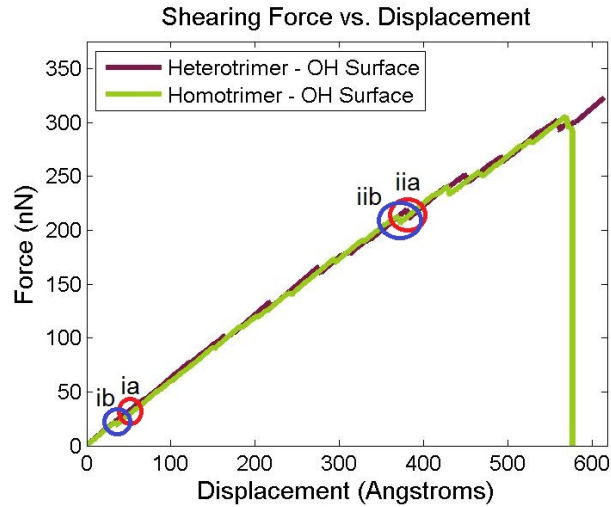


**Figure 11: Locations of First and Final Slips: ia) First slip for heterotrimer, ib) First slip for homotrimer, iia) Final slip for heterotrimer, iib) Final slip for homotrimer**

Figure 11 above shows the locations of the first and final slips of the shearing system. The red circles represent the locations of heterotrimeric collagen slips, while the blue circles represent the locations of homotrimeric collagen slips. Below, a careful look is taken for each location.

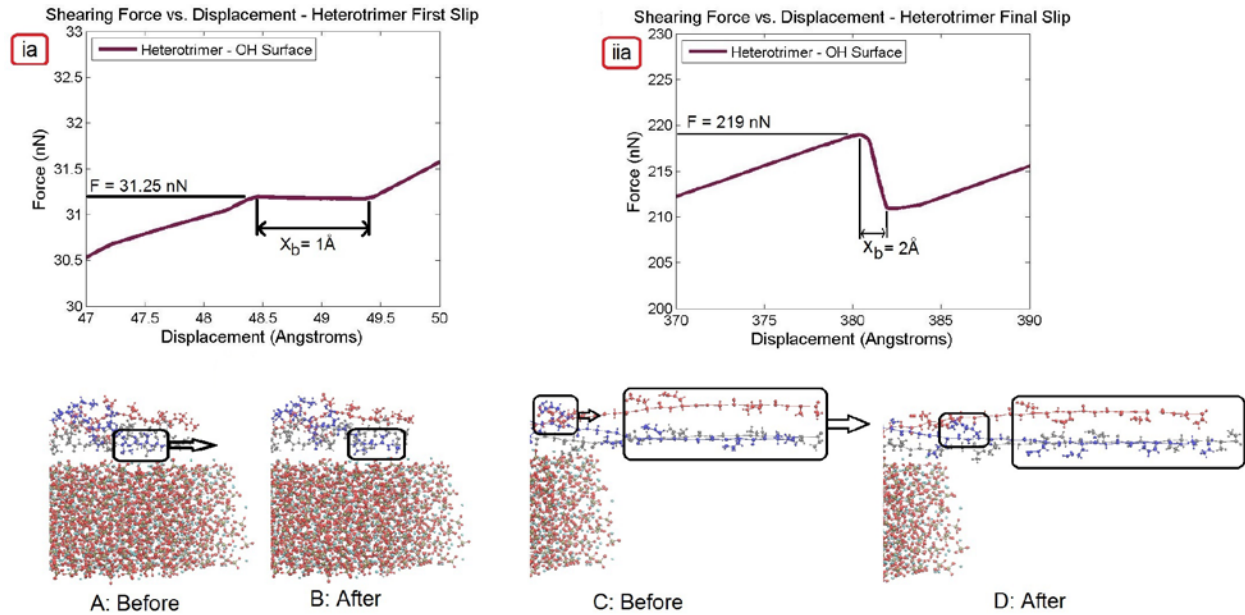


**Figure 12: Zoomed-In Heterotrimeric Slip Force vs. Displacement: ia) Location of first slip, iia) Location of final slip, A) Image from before first slip, B) Image from after first slip, C) Image from before final slip, D) Image from after final slip.**

As can be seen in the figure above, the final slip creates a greater drop in force than the first slip. This is because the forces at lower displacements are enough to break bonds, but not

strong enough to create huge slips of the collagen. In the top left panel (ia.) the rupture force,  $F$ , is 31.25 nN at a rupture distance,  $x_b$ , of 1 Å while the top right panel (iia.) has a rupture force of 219 nN over a distance of 2 Å. The lower left panels show the extent of the first slip in the heterotrimeric system.

We apply the Bell model to the locations highlighted above and calculate the following energy barriers for heterotrimeric collagen.

Location	Energy Barrier ( $\frac{kcal}{mol}$ )
<b>ia: First Slip for Heterotrimer</b>	<b>468 kcal/mol</b>
<b>iia: Final Slip for Heterotrimer</b>	<b>6320 kcal/mol</b>

**Table 2: Energy barriers associated with the first and final slips in the heterotrimeric collagen system**

As shown in the table above, the energy barrier is considerably increased for slips that occur at higher forces. The number of hydrogen bonds associated with this much energy must come from the water-water hydrogen bonds breaking, because there aren't enough bonds formed to the collagen itself to produce this much energy. Below we look at the homotrimeric collagen system to analyze the energy barriers of the hydrogen bonds during the first slip and the final slip.

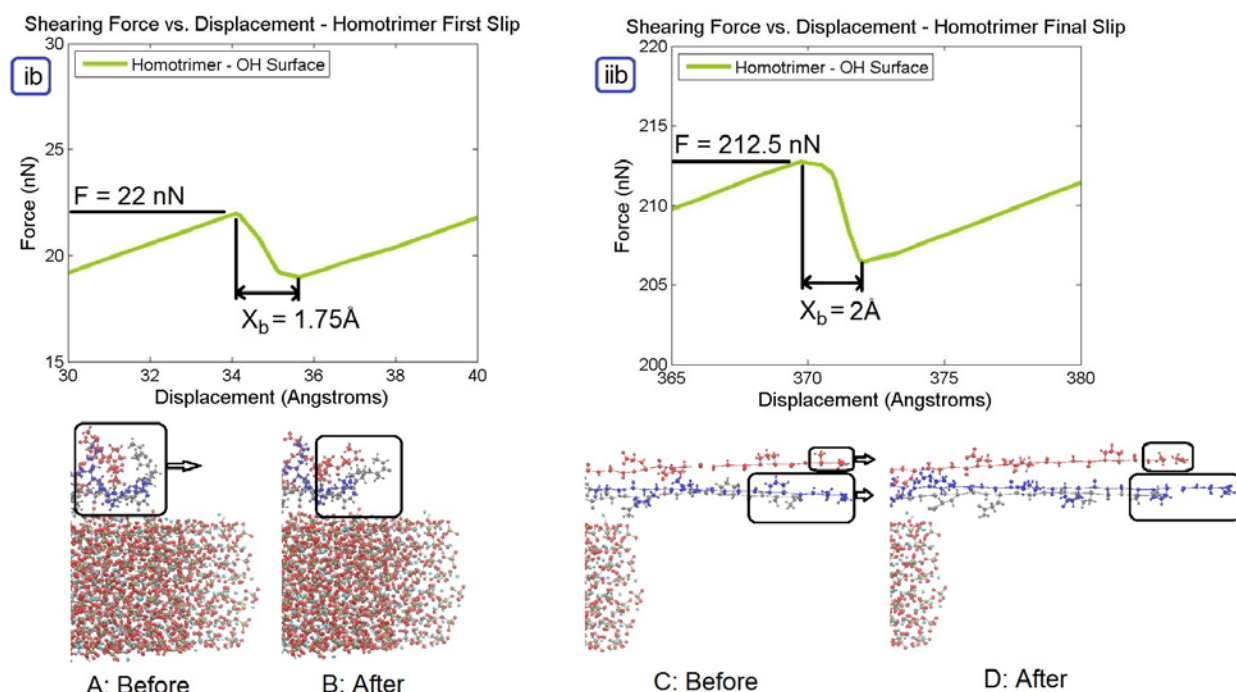


**Figure 13: Zoomed-In Homotrimeric Slip Force vs. Displacement: ia) Location of first slip, iia) Location of final slip, A) Image from before first slip, B) Image from after first slip, C) Image from before final slip, D) Image from after final slip.**

As shown in the figure above, the first slip of the homotrimeric system produces a greater drop in force than the first slip in the heterotrimeric system. This is because the end of the homotrimeric collagen has slightly coiled up on itself during equilibration. Figure 13A shows

this slight coiling, while B shows the collagen after. The final slip of the homotrimeric system is very similar to the final slip shown in figure 12 C,D.

Location	Energy Barrier ( $\frac{kcal}{mol}$ )
ia: First Slip for Homotrimer	572 kcal/mol
iiia: Final Slip for Homotrimer	6130 kcal/mol

**Table 3: Energy barriers associated with the first and final slips in the homotrimeric collagen system**

Table 3 above shows the two energy barriers that coincide with the first slip and the final slip of the system. An interesting note about the nature of the Bell model is that even though less force is involved in the first slip of the homotrimeric collagen system, the energy barrier is higher due to increased rupture distance. The energy barrier of the final slip of the homotrimeric system is very similar to the final slip of the heterotrimeric system, but when examining figure 11 it is evident that the heterotrimeric system experiences more major slips, whereas the homotrimeric system is smoother. This can be explained by the fact that the homotrimeric collagen forms considerably fewer hydrogen bonds than the heterotrimeric collagen.

#### 4.2.1 Peeling of Heterotrimeric and Homotrimeric Collagen-HAP

We simulate the peeling systems using SMD for approximately 42 ns. During this time the forces reach a maximum of 215 nN for homotrimeric collagen and 210 nN for heterotrimeric collagen before finally uncoiling and rupturing from the surface. This is shown below in figure 14.

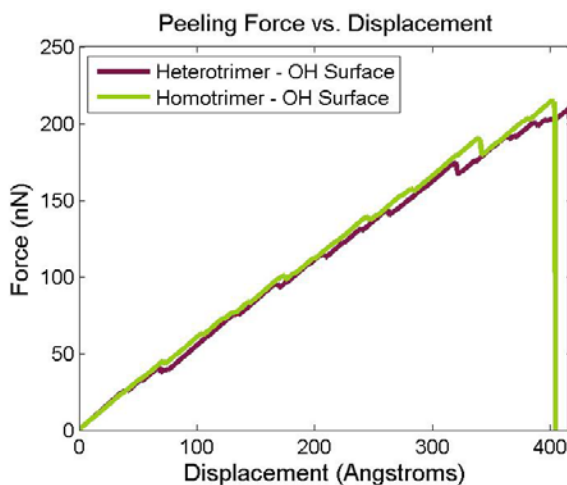


**Figure 14: Force vs. Displacement of Heterotrimeric and Homotrimeric Collagen**

Figure 14 above shows the force vs. displacement for the peeling system. As can immediately be seen in the figure above, the presence of mutated collagen has no effect on the overall trajectory of peeling displacement. Looking at low displacements provides us with insight into the stiffness of the interface and information about the first bonds that break.



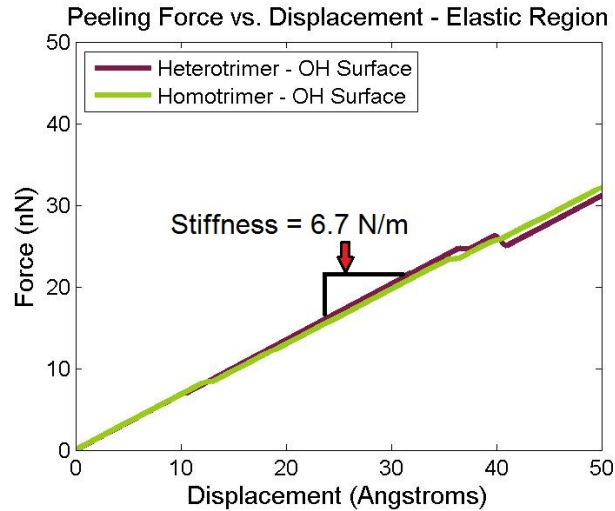


**Figure 15: Force vs. Displacement in Elastic Region of Peeling System**

Figure 15 above shows the force vs. displacement for the region of low displacement. Comparing this to figure 7 shows that both systems exhibit the same initial stiffness. This could occur due to the static nature of hydrogen bonds. The system never moves at a steady rate. It can only form, break, and reform bonds to reach new points of equilibrium. The bonds associated with the static equilibrium of both systems must be identical. Below we look at the hydrogen bonds that the collagen forms with itself, HAP, and water to get a better understanding of the system as a whole.

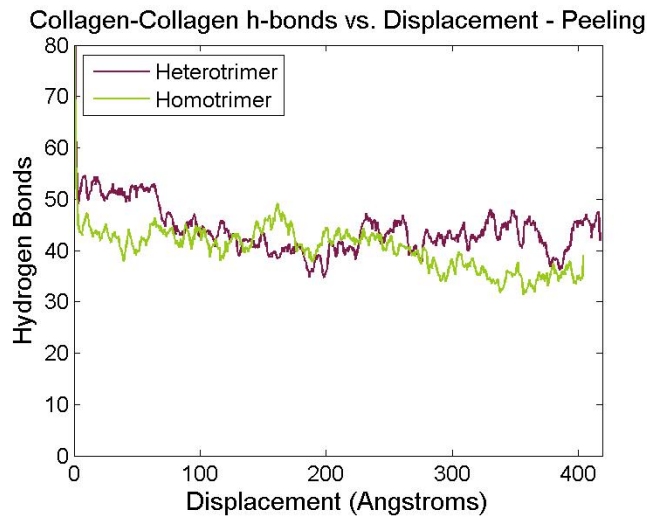


**Figure 16: Collagen-Collagen Hydrogen Bonds vs. Displacement for Peeling**

Figure 16 above shows the plot of collagen-collagen hydrogen bonds formed during the SMD simulation. Interestingly, the homotrimeric collagen forms about 20% fewer collagen-collagen hydrogen bonds at low displacements, but this trend quickly equalizes after about 70Å of displacement. After this point, the number of collagen-collagen hydrogen bonds remains similar across systems until about 220Å when homotrimeric collagen starts a downward trend

while heterotrimeric collagen remains constant. This may help explain why the homotrimeric collagen ruptures before the heterotrimeric collagen.

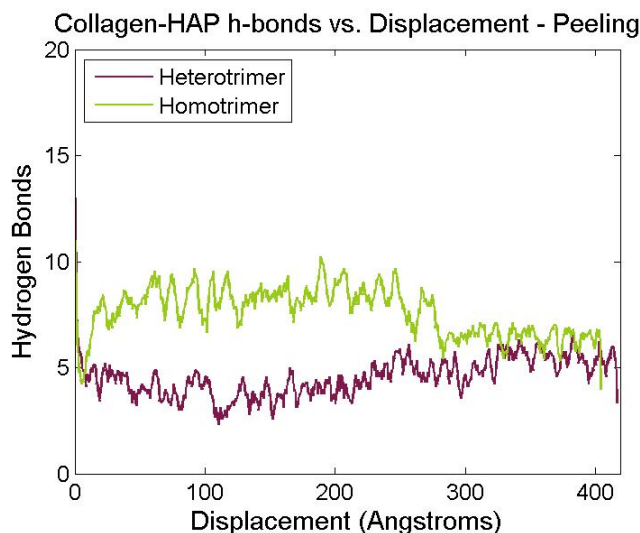


**Figure 17: Collagen-HAP Hydrogen Bonds vs. Displacement for Peeling**

Figure 17 above shows the plot of hydrogen bonds formed between the collagen and HAP during the SMD simulation. Interestingly, the homotrimeric collagen from the shearing system forms 40% fewer collagen-collagen bonds than its peeling counterpart. This result is odd, because the two systems should be very similar at the start of the SMD simulation, only deviating after enough force has been applied to break the first bonds. Figure 17 also highlights the difference that mutation makes regarding collagen-collagen bonds. Homotrimeric collagen in the peeling system forms about 100% more bonds than heterotrimeric collagen until about 270Å displacement where the gap is narrowed to less than 20%.

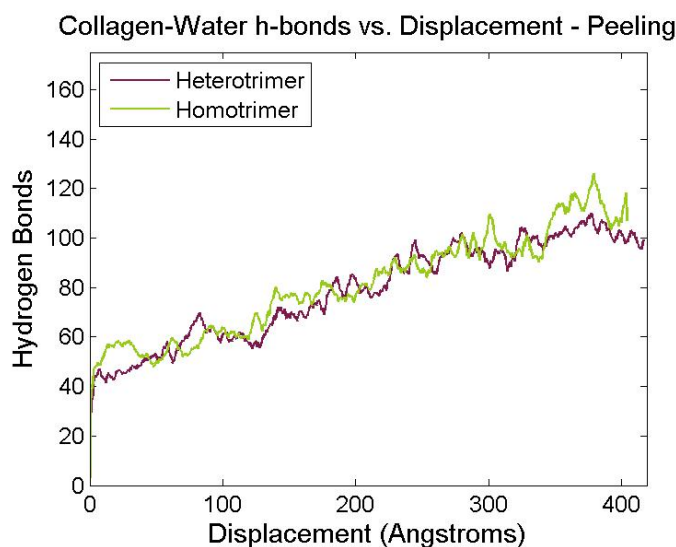


**Figure 18: Collagen-Water Hydrogen Bonds vs. Displacement for Peeling**

Figure 18 above shows the hydrogen bonds formed between the collagen and the water. There is no real difference in trend between the homotrimeric and heterotrimeric collagen. It is interesting to note the oscillations present in the plot. Even with a moving average applied to the hydrogen bonds, there are waves occurring over lengths of about 10 Å. This means that bonds are constantly breaking and reforming as the sample is pulled by the spring. Comparing this plot to figure 10 shows nearly identical overall trends of increasing collagen-water bonds as the collagen separates and uncoils. This is directly related to more exposed atoms in the uncoiled sections of collagen.

#### 4.3 Biologically Inspired Materials Based on Collagen-HAP System

This research has inspired us to design a 3D model of the collagen-HAP system and print it using an ABS plastic additive printer. When conducting simulations on the system we noticed the geometric shapes that the OH channels form along with the smaller channels formed through the Ca surface. Below is a labelled snapshot highlighting the hexagonal OH channels.

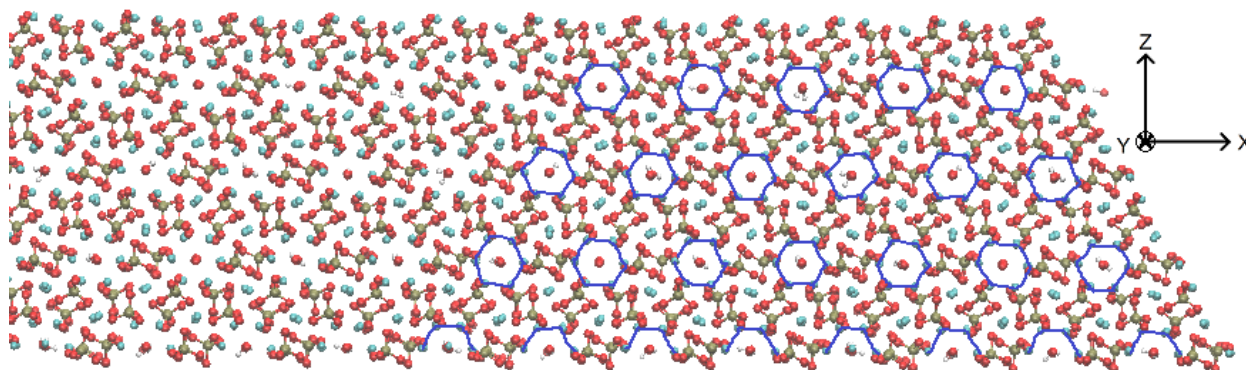


**Figure 19: HAP OH-Surface Highlighted to show hexagonal channels**

Figure 19 above depicts how the OH channels take the shape of hexagons through the HAP cells. These channels run completely through the HAP in the face. The blue hexagons drawn highlight the borders of these channels. The calcium atoms form the corners of the channel.

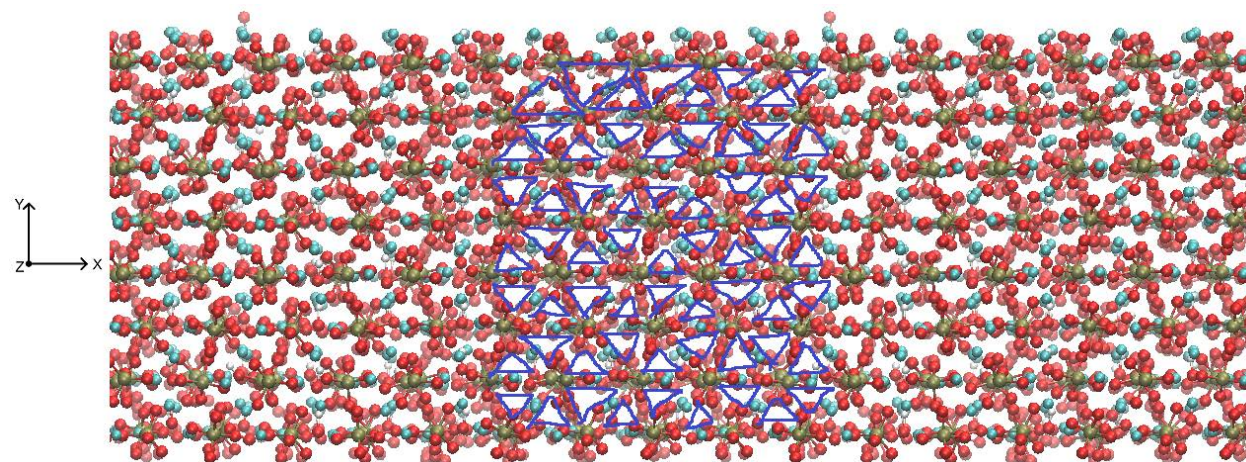


**Figure 20: HAP Ca-Surface Highlighted to show triangular channels**

Figure 20 above shows a snapshot of the Ca-surface of HAP with the triangular channels highlighted using blue triangles. These channels are particularly interesting, because the position and orientation of the triangles appears to be broken down hexagons. This shows that HAP crystal must obtain its strength and rigidity through these geometric organizations. We combined the two observations to produce the model shown below



**Figure 21: 3D Printed Collagen-HAP System**

Figure 21 above shows the final design of the bio-inspired 3D model. The top surface contains multiple hexagons that represent the OH channels seen in real HAP crystals.

## **5. Conclusions**

We use SMD simulations to study the force displacement behavior of heterotrimeric and homotrimeric collagen, when interacting with HAP under shear and peeling loading conditions. We use Bell model to predict the energy barrier of several mechanisms under shear loading. The conclusions of our study are listed below.

1. Heterotrimeric collagen and homotrimeric collagen follow nearly identical force vs. displacement paths in the elastic region for the shear and peeling cases. This implies that at this scale mutations do not have a significant effect for the system studied here.
2. During shear test, the homotrimeric collagen forms considerably fewer hydrogen bonds overall compared to heterotrimeric collagen. This implies that homotrimeric collagen is weak in shear, however the hydrogen bonds formed with water is approximately the same for both types of collagen, which explains the force displacement behavior.
3. Under shear loading the number of collagen-HAP hydrogen bonds formed for homotrimeric collagen is less than heterotrimeric collagen, which implies that the heterotrimeric collagen has better resistance to shear deformation on HAP surface.
4. The Bell model predicts the energy barriers associated with key mechanisms (e.g. collagen uncoiling) of both homotrimer and heterotrimeric under shear force. The energy barriers calculated using this model could be used for macroscale models of bone to define failure criteria.
5. Materials and objects can be designed based on the nanostructure of HAP. Geometrically optimized channels in HAP led to the development of a macroscale 3D printed model of the entire system.

## **Acknowledgements**

Many thanks to Dr. Arun K. Nair for helping me solve the unsolvable and get through the end of this semester. Without his guidance and support I would never have come close to accomplishing as much as I did. I want to also thank the Arkansas High Performance Computing Center for allowing me to store countless amounts of data on their servers and perform simulations spanning over weeks.



## References

1. Plimpton, S., *Fast Parallel Algorithms for Short-Range Molecular-Dynamics*. Journal of Computational Physics, 1995. **117**(1): p. 1-19.
2. Rauch, F. and F.H. Glorieux, *Osteogenesis imperfecta*. Lancet, 2004. **363**(9418): p. 1377-1385.
3. Foundation, O.I. *Testing for Osteogenesis Imperfecta*. [Web] 2007 4/11/2015 [cited 2015 4/11/2015]; Available from: <http://www.oif.org/site/PageServer?pagename=Testing>.
4. Launey, M.E., M.J. Buehler, and R.O. Ritchie, *On the Mechanistic Origins of Toughness in Bone*. Annual Review of Materials Research, Vol 40, 2010. **40**: p. 25-53.
5. Fratzl, P., H.S. Gupta, E.P. Paschalis, and P. Roschger, *Structure and mechanical quality of the collagen-mineral nano-composite in bone*. Journal of Materials Chemistry, 2004. **14**(14): p. 2115-2123.
6. Gupta, H.S., J. Seto, W. Wagermaier, P. Zaslansky, P. Boesecke, and P. Fratzl, *Cooperative deformation of mineral and collagen in bone at the nanoscale*. Proceedings of the National Academy of Sciences of the United States of America, 2006. **103**(47): p. 17741-17746.
7. Weiner, S. and H.D. Wagner, *The material bone: Structure mechanical function relations*. Annual Review of Materials Science, 1998. **28**: p. 271-298.
8. Ji, B.H. and H.J. Gao, *Mechanical properties of nanostructure of biological materials*. Journal of the Mechanics and Physics of Solids, 2004. **52**(9): p. 1963-1990.
9. Nair, A.K., A. Gautieri, S.W. Chang, and M.J. Buehler, *Molecular mechanics of mineralized collagen fibrils in bone*. Nature Communications, 2013. **4**.
10. Ackbarow, T. and M.J. Buehler, *Alpha-helical protein domains unify strength and robustness through hierarchical nanostructures*. Nanotechnology, 2009. **20**(7).
11. Mirzaeifar, R., Z. Qin, and M.J. Buehler, *Tensile strength of carbyne chains in varied chemical environments and structural lengths*. Nanotechnology, 2014. **25**(37).
12. Qin, Z., S. Cranford, T. Ackbarow, and M.J. Buehler, *Robustness-Strength Performance of Hierarchical Alpha-Helical Protein Filaments*. International Journal of Applied Mechanics, 2009. **1**(1): p. 85-112.
13. Chang, S.W., S.J. Shefelbine, and M.J. Buehler, *Structural and Mechanical Differences between Collagen Homo- and Heterotrimers: Relevance for the Molecular Origin of Brittle Bone Disease*. Biophysical Journal, 2012. **102**(3): p. 640-648.
14. Rainey, J.K. and M.C. Goh, *An interactive triple-helical collagen builder*. Bioinformatics, 2004. **20**(15): p. 2458-2459.
15. Libonati, F., A.K. Nair, L. Vergani, and M.J. Buehler, *Mechanics of collagen-hydroxyapatite model nanocomposites*. Mechanics Research Communications, 2014. **58**: p. 17-23.
16. Humphrey, W., A. Dalke, and K. Schulten, *VMD: Visual molecular dynamics*. Journal of Molecular Graphics & Modelling, 1996. **14**(1): p. 33-38.
17. Libonati, F., A.K. Nair, L. Vergani, and M.J. Buehler, *Fracture mechanics of hydroxyapatite single crystals under geometric confinement*. Journal of the Mechanical Behavior of Biomedical Materials, 2013. **20**: p. 184-191.
18. Qin, Z., A. Gautieri, A.K. Nair, H. Inbar, and M.J. Buehler, *Thickness of Hydroxyapatite Nanocrystal Controls Mechanical Properties of the Collagen-Hydroxyapatite Interface*. Langmuir, 2012. **28**(4): p. 1982-1992.

19. Park, S., R.J. Radmer, T.E. Klein, and V.S. Pande, *A new set of molecular mechanics parameters for hydroxyproline and its use in molecular dynamics simulations of collagen-like peptides*. Journal of Computational Chemistry, 2005. **26**(15): p. 1612-1616.
20. Bhowmik, R., K.S. Katti, and D. Katti, *Molecular dynamics simulation of hydroxyapatite-polyacrylic acid interfaces*. Polymer, 2007. **48**(2): p. 664-674.
21. Hauptmann, S., H. Dufner, J. Brickmann, S.M. Kast, and R.S. Berry, *Potential energy function for apatites*. Physical Chemistry Chemical Physics, 2003. **5**(3): p. 635-639.
22. Dubey, D.K. and V. Tomar, *Role of the nanoscale interfacial arrangement in mechanical strength of tropocollagen-hydroxyapatite-based hard biomaterials*. Acta Biomaterialia, 2009. **5**(7): p. 2704-2716.
23. Shen, J.W., T. Wu, Q. Wang, and H.H. Pan, *Molecular simulation of protein adsorption and desorption on hydroxyapatite surfaces*. Biomaterials, 2008. **29**(5): p. 513-532.
24. Gautieri, A., S. Uzel, S. Vesentini, A. Redaelli, and M.J. Buehler, *Molecular and Mesoscale Mechanisms of Osteogenesis Imperfecta Disease in Collagen Fibrils*. Biophysical Journal, 2009. **97**(3): p. 857-865.
25. Dubey, D.K. and V. Tomar, *Effect of osteogenesis imperfecta mutations in tropocollagen molecule on strength of biomimetic tropocollagen-hydroxyapatite nanocomposites*. Applied Physics Letters, 2010. **96**(2).